

Supplement of Atmos. Chem. Phys., 16, 5573–5594, 2016
<http://www.atmos-chem-phys.net/16/5573/2016/>
doi:10.5194/acp-16-5573-2016-supplement
© Author(s) 2016. CC Attribution 3.0 License.



Atmospheric
Chemistry
and Physics
Open Access
EGU

Supplement of

Aerosol–radiation–cloud interactions in a regional coupled model: the effects of convective parameterisation and resolution

Scott Archer-Nicholls et al.

Correspondence to: G. McFiggans (g.mcfiggans@manchester.ac.uk)

The copyright of individual parts of the supplement might differ from the CC-BY 3.0 licence.

Supplementary material for:

Aerosol–radiation–cloud interactions in a regional coupled model: the effects of convective parameterisation and resolution

Scott Archer-Nicholls^{1,*}, Douglas Lowe¹, David M. Schultz¹, and Gordon McFiggans¹

¹Centre for Atmospheric Sciences, School of Earth, Atmospheric and Environmental Sciences, University of Manchester, Manchester, UK

*Now at: National Centre for Atmospheric Research (NCAR), Boulder, CO, USA

Correspondence to: Gordon McFiggans (g.mcfiggans@manchester.ac.uk)

This document serves as a description of the supplementary material for the above paper. Tables 1-3 show summaries of domain averaged statistics of diagnostic radiative variables for each of the scenarios for each case study. Tables 4-6 are similar tables showing temperature at 2m above surface, planetary boundary layer height and precipitation.

Figures 1 and 2 are equivalent figures to Figure 4 in the main paper, for the other two case study days (18 and 23 September respectively). These were not included in the main paper due to their similarity to the first case study day (14 September), but have been included here for completeness. Figure 3 in this supplement is complimentary to Figure 5 in the main paper, showing down-welling SW radiation at the surface, including the effects of clouds for each case study day.

The changes in cloud cover and precipitation over all scenarios on 18 September are presented in Figure 4, demonstrating the impact of not using a convective parameterisation. Total cloud cover is marginally reduced in the local afternoon without the convective parameterisation. However, the clearest effect is that there is a large reduction in ice clouds at night. Deep convective towers are smaller and take longer to form without a convective parameterisation, delaying the onset of and reducing total precipitation.

Total cloud cover is marginally reduced in the local afternoon without the convective parameterisation. However, the clearest effect is that there is a large reduction in ice clouds at night (Fig. 4). Deep convective towers are smaller and take longer to form without a convective parameterisation, delaying the onset of and reducing total precipitation. The FE_nCU

scenario has slightly increased precipitation at night compared to nFE_nCU, whereas the FE scenario has less precipitation over the entire day compared to nFE (Fig. 4c).

The 1km domain receives a greater portion of SW radiation at the surface, compared to the same region of the 5km domain, as shown in Figure 5. Likewise, the net radiative balance is strongly positive in the 1km domain. This demonstrates the impact of reduced cloud cover on radiative fields in the 1km domain.

The runs without convective parameterisation have reduced deep convection in the local afternoon, resulting in more downwelling SW radiation at the surface (Fig. 6a). The change in surface SW radiation at local afternoon is approximately twice as sensitive to the use of convective parameterisation to the presence of BBA. The reduction of high-altitude nighttime ice clouds when running without the convective parameterisation creates an extremely strong negative forcing at night as more LW radiation is lost to space in the runs without convective parameterization (Fig 6b).

Overall, RB is more sensitive to whether or not a convective parameterisation is used than it is to the presence of aerosol or the horizontal resolution. The diurnally averaged reduction of RB is approximately 20 Wm^{-2} between scenarios with and without convective parameterisation (Table S2 in the Supplement). This change is largely due to the reduction in nighttime clouds in the runs without convective parameterisation.

Changes in cloud cover due to the presence of aerosol have a smaller impact on the net radiative balance on the 1 km domain, resulting in lower magnitude of changes to the radiative budget (Fig. 7). The 1 km domain is sensitive to the boundary conditions from the 5 km domain, highlighted by the similarity in nighttime radiative balance changes due to ice clouds between the 1 km domain and same region covered by the 5 km domain (Fig. 7a and b). Precipitation is strongly suppressed over the 1 km region in the 5 km domain in the scenarios where convective parameterisation is turned off (Fig 6c and d). More precipitation is produced in the 1 km domain for these runs, although still less than in the scenarios with convective parameterisation over the 5 km domain, highlighting the importance of the boundary conditions from the 5 km in determining the behavior of the 1 km domain. In contrast, the runs with convective parameterisation turned on produce similar amounts of precipitation at both resolutions, implying that a convective parameterisation may be needed over the 5 km domain to produce reasonable levels of precipitation.

Table 1. Summary of radiative flux statistics for 14 September case study. Mean down-welling SW radiation at surface ($SW\downarrow_{sfc}$), radiative balance (RB) and absorbed SW radiation (ASW), averaged over 5-km domain, the 1-km region of the 5-km domain, and the 1-km domain, all in units $W\ m^{-2}$. Uncertainties show standard deviation across domain. Averaged over 24 hours, from dawn to dawn, between 10:00~UTC 14 and 10:00~UTC 15 September.

Scenario	$SW\downarrow_{sfc}$			RB			ASW		
	5-km	5-km over 1-km	1-km	5-km	5-km over 1-km	1-km	5-km	5-km over 1-km	1-km
FE	220±33	226± 8	226±10	64±46	53± 9	53± 9	134±11	137± 6	137± 7
nFE	254±37	269±11	270±11	65±49	55±15	56±15	106± 6	104± 2	104± 2
nARI	272±45	285±21	289±19	66±54	55±22	58±21	92± 5	91± 2	91± 2
Ctrl	272±45	285±21	289±19	66±54	55±21	58±21	92± 5	91± 2	91± 2

Table 2. Summary of radiative flux statistics for 18 September case study. Mean down-welling SW radiation at surface ($SW_{\downarrow sfc}$), radiative balance (RB) and absorbed SW radiation (ASW), averaged over 5-km domain, the 1-km region of the 5-km domain, and the 1-km domain, all in units $W m^{-2}$. Uncertainties show standard deviation across domain. Averaged over 24 hours, from dawn to dawn, between 10:00 UTC 18 and 10:00 UTC 19 September.

Scenario	$SW_{\downarrow sfc}$			RB			ASW		
	5-km	5-km over 1-km	1-km	5-km	5-km over 1-km	1-km	5-km	5-km over 1-km	1-km
FE	224±42	215±33	227±34	92±60	72±35	78±36	123±10	129± 8	130± 9
nFE	243±48	239±44	255±46	94±66	82±48	88±50	104± 6	103± 4	103± 5
nARI	253±53	243±47	264±50	93±69	75±49	87±52	95± 6	95± 4	94± 4
Ctrl	253±53	245±47	263±49	94±69	82±50	90±53	95± 6	95± 4	94± 4
FE_nCU	233±39	230±22	234±23	71±50	56±22	59±23	125±10	131± 8	130± 8
nFE_nCU	255±46	262±29	267±32	71±57	56±29	62±31	106± 6	104± 3	103± 4
nARI_nCU	267±52	273±35	281±35	71±61	57±34	64±35	97± 6	96± 3	95± 3
Ctrl_nCU	267±52	273±34	280±36	72±61	57±33	64±36	97± 6	96± 3	95± 3

Table 3. Summary of radiative flux statistics for 23 September case study. Mean down-welling SW radiation at surface ($SW\downarrow_{sfc}$), radiative balance (RB) and absorbed SW radiation (ASW), averaged over 5-km domain, the 1-km region of the 5-km domain, and the 1-km domain, all in units $W\ m^{-2}$. Uncertainties show standard deviation across domain. Averaged over 24 hours, from dawn to dawn, between 10:00 UTC 23 and 10:00 UTC 24 September.

Scenario	$SW\downarrow_{sfc}$			RB			ASW		
	5-km	5-km over 1-km	1-km	5-km	5-km over 1-km	1-km	5-km	5-km over 1-km	1-km
FE	214±58	242±26	242±30	112±69	96±28	95±31	122±12	117± 6	117± 7
nFE	235±65	263±31	263±35	114±74	102±34	101±37	103± 9	101± 4	101± 5
nARI	243±71	275±34	275±38	112±77	103±34	103±37	96± 8	94± 4	94± 4
Ctrl	244±70	273±35	274±38	114±77	104±37	104±40	96± 8	94± 4	94± 5

Table 4. Summary of meteorological and dynamical variable statistics for 14 September case study. Mean temperature at two meters above surface (T_2), planetary boundary layer height, as calculated by the YSU PBL parameterisation (PBLH), and accumulated precipitation. Averaged over 5-km domain, the 1-km region of the 5-km domain, and the 1-km domain. Uncertainties show standard deviation across domain. Averaged or accumulated over 24 hours, from dawn to dawn, between 10:00 UTC 14 and 10:00 UTC 15 September.

Scenario	T_2 (°C)			PBLH (m)			Precipitation (mm)		
	5-km	5-km over 1-km	1-km	5-km	5-km over 1-km	1-km	5-km	5-km over 1-km	1-km
FE	30.4±0.9	30.9±0.4	30.8±0.6	681±235	661±92	594±159	0.49±0.59	0.01±0.05	0.00±0.00
nFE	30.7±1.0	31.4±0.4	31.3±0.6	779±243	819±108	725±191	0.54±0.60	0.04±0.11	0.00±0.00
nARI	30.9±1.0	31.5±0.4	31.4±0.6	838±261	886±109	797±205	0.58±0.61	0.08±0.16	0.00±0.04
Ctrl	30.9±1.0	31.5±0.4	31.4±0.6	837±259	892±109	798±207	0.57±0.61	0.08±0.14	0.01±0.05

Table 5. Summary of meteorological and dynamical variable statistics for 18 September case study. Mean temperature at two meters above surface (T_2), planetary boundary layer height, as calculated by the YSU PBL parameterisation (PBLH), and accumulated precipitation. Averaged over 5-km domain, the 1-km region of the 5-km domain, and the 1-km domain. Uncertainties show standard deviation across domain. Averaged or accumulated over 24 hours, from dawn to dawn, between 10:00 UTC 18 and 10:00 UTC 19 September.

Scenario	T_2 (°C)			PBLH (m)			Precipitation (mm)		
	5-km	5-km over 1-km	1-km	5-km	5-km over 1-km	1-km	5-km	5-km over 1-km	1-km
FE	29.2±0.9	29.3±0.6	29.4±0.7	741±245	733±187	720±215	2.50±2.49	1.89±1.62	2.30±4.13
nFE	29.3±1.0	29.4±0.5	29.4±0.7	761±255	732±170	695±225	3.09±3.09	2.72±1.38	3.14±4.19
nARI	29.4±1.0	29.5±0.6	29.5±0.8	778±254	754±176	713±238	3.11±3.11	2.70±1.62	3.95±5.12
Ctrl	29.3±1.0	29.4±0.6	29.4±0.8	772±256	741±166	702±234	3.23±3.18	3.03±1.46	3.72±4.54
FE_nCU	29.3±1.0	29.7±0.4	29.6±0.6	774±260	781±155	723±191	1.58±4.14	0.51±1.04	1.16±2.25
nFE_nCU	29.5±1.0	29.9±0.4	29.8±0.6	801±275	793±160	727±204	1.58±4.11	0.66±1.40	1.46±2.13
nARI_nCU	29.6±1.0	30.1±0.4	30.0±0.6	815±281	827±169	752±209	1.72±3.95	0.61±1.27	1.67±2.20
Ctrl_nCU	29.6±1.1	30.1±0.4	29.9±0.6	814±282	834±165	742±206	1.73±4.40	0.58±1.18	1.77±2.56

Table 6. Summary of meteorological and dynamical variable statistics for 23 September case study. Mean temperature at two meters above surface (T_2), planetary boundary layer height, as calculated by the YSU PBL parameterisation (PBLH), and accumulated precipitation. Averaged over 5-km domain, the 1-km region of the 5-km domain, and the 1-km domain. Uncertainties show standard deviation across domain. Averaged or accumulated over 24 hours, from dawn to dawn, between 10:00 UTC 23 and 10:00 UTC 24 September.

Scenario	T_2 (°C)			PBLH (m)			Precipitation (mm)		
	5-km	5-km over 1-km	1-km	5-km	5-km over 1-km	1-km	5-km	5-km over 1-km	1-km
FE	27.2±1.0	27.6±0.3	27.5±0.4	487±174	554±75	503±115	5.22±7.56	0.00±0.03	0.00±0.02
nFE	27.4±1.1	27.9±0.3	27.8±0.4	522±192	587±80	537±124	5.74±7.93	0.01±0.03	0.00±0.01
nARI	27.4±1.1	28.0±0.3	28.0±0.4	530±197	605±77	557±127	5.11±6.80	0.00±0.03	0.00±0.02
Ctrl	27.4±1.1	28.0±0.3	27.9±0.4	533±198	600±79	553±127	5.57±7.20	0.00±0.01	0.00±0.01

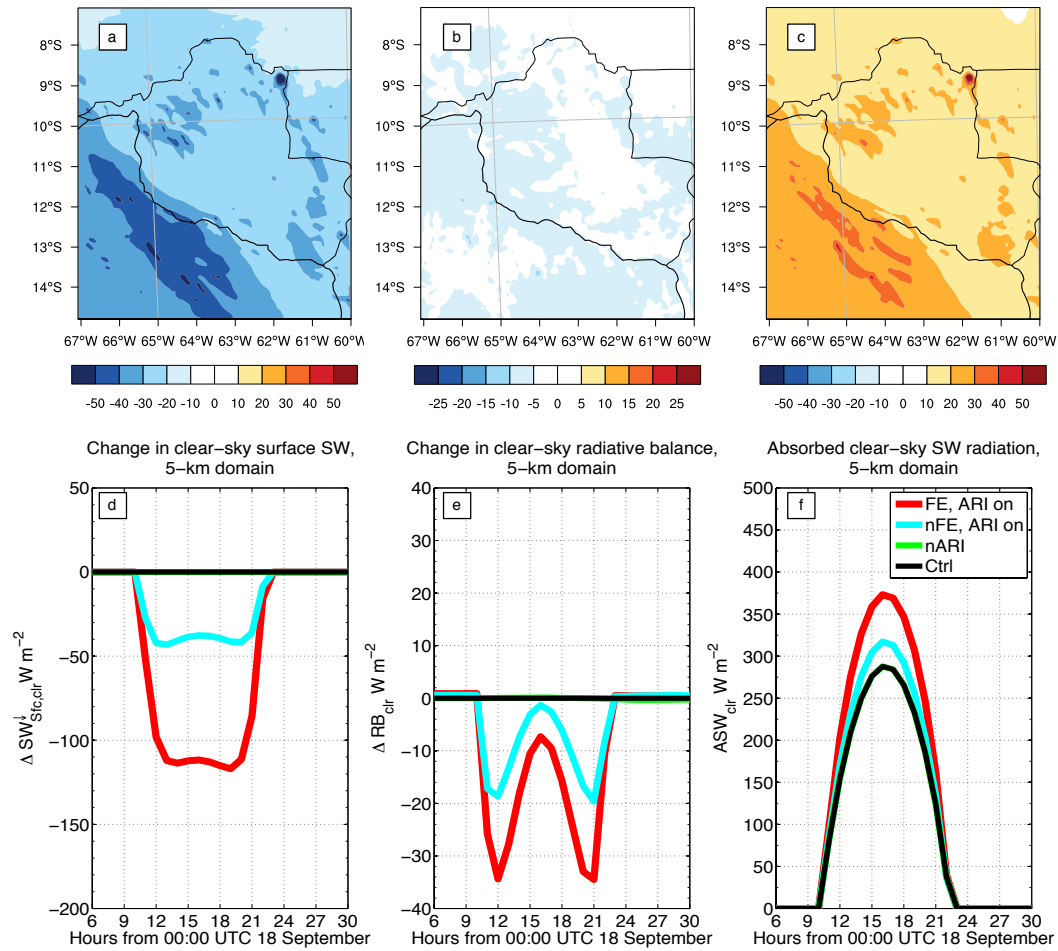


Figure 1. Maps and time-series of changes to clear-sky radiation fields (ignoring the effects of clouds) due to BBA over 18 September 2012. (a-c) show maps over 5-km domain of the difference between the FE and nFE scenarios, averaged over 24 hours, from dawn to dawn, between 10:00 UTC 18 and 10:00 UTC 19 September. (d-f) show model output averaged over the 5-km domain at each hour of simulation for the FE, nFE, nARI and Ctrl scenarios; with (d) and (e) plotting difference from Ctrl scenario. (a) and (d) change in downwelling SW radiation at the surface. (b) and (e) change in radiative balance at TOA. (c) and (f) SW radiation absorbed by the atmospheric column. Calculations of derived variables are explained in Appendix A. All variables are in units $W m^{-2}$.

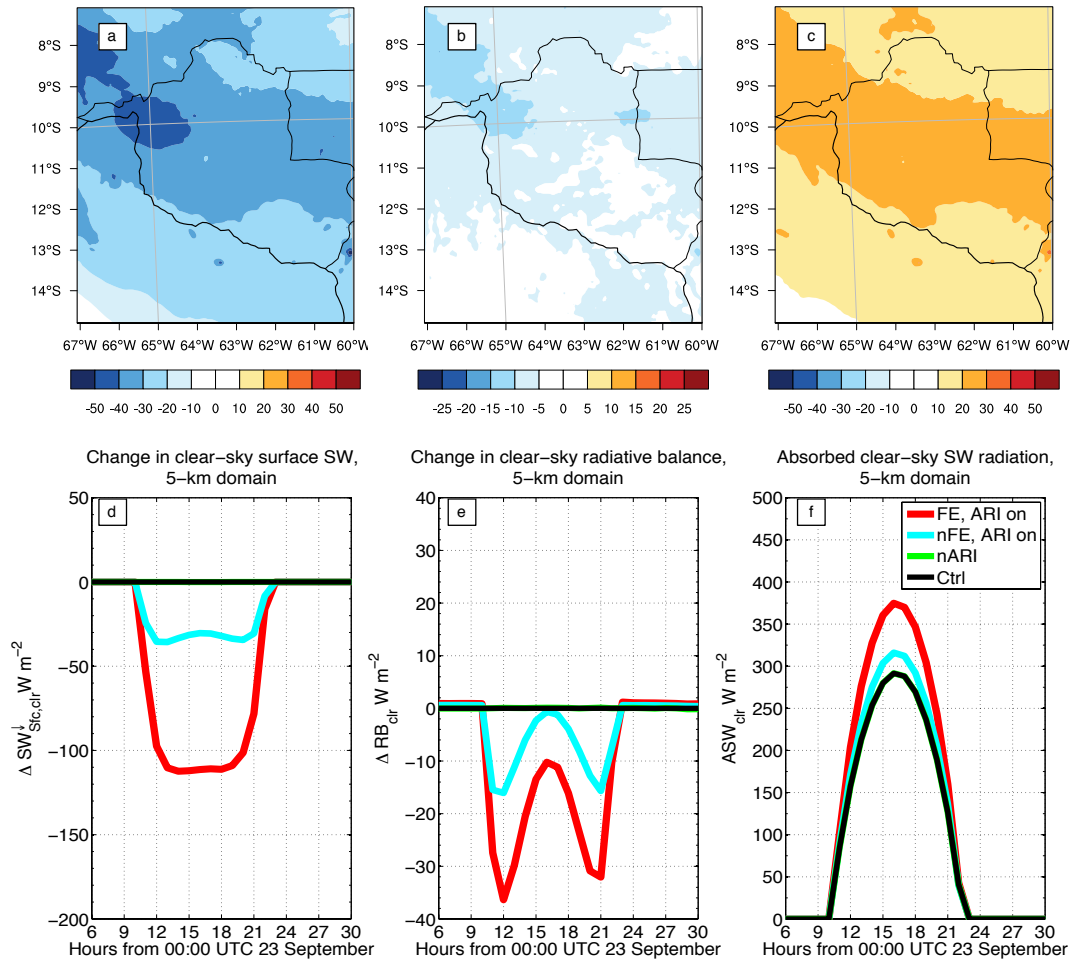


Figure 2. Maps and time-series of changes to clear-sky radiation fields (ignoring the effects of clouds) due to BBA over 23 September 2012. (a-c) show maps over 5-km domain of the difference between the FE and nFE scenarios, averaged over 24 hours, from dawn to dawn, between 10:00 UTC 23 and 10:00 UTC 24 September. (d-f) show model output averaged over the 5-km domain at each hour of simulation for the FE, nFE, nARI and Ctrl scenarios; with (d) and (e) plotting difference from Ctrl scenario. (a) and (d) change in downwelling SW radiation at the surface. (b) and (e) change in radiative balance at TOA. (c) and (f) SW radiation absorbed by the atmospheric column. Calculations of derived variables are explained in Appendix A. All variables are in units $W m^{-2}$.

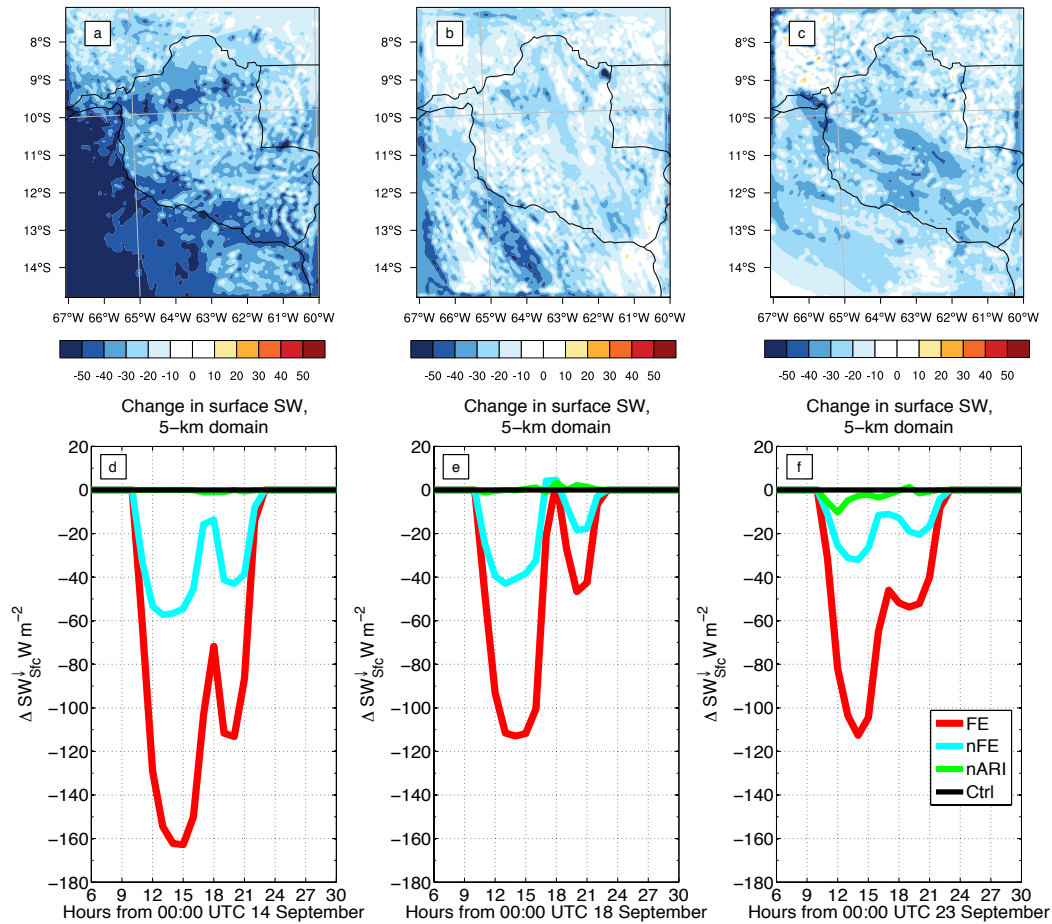


Figure 3. Maps and time-series of changes to downwelling SW radiation at surface for each of the three case study days, including the effects of clouds. (a-c) show maps over 5-km domain of the difference between the FE and nFE scenarios, averaged over 24 hours, from dawn to dawn, from 10:00 UTC, for (a) 14 September, (b) 18 September and (c) 23 September. (d-f) time series of downwelling SW radiation at surface averaged over 5-km domain at each hour of simulation. All variables are in units $W m^{-2}$.

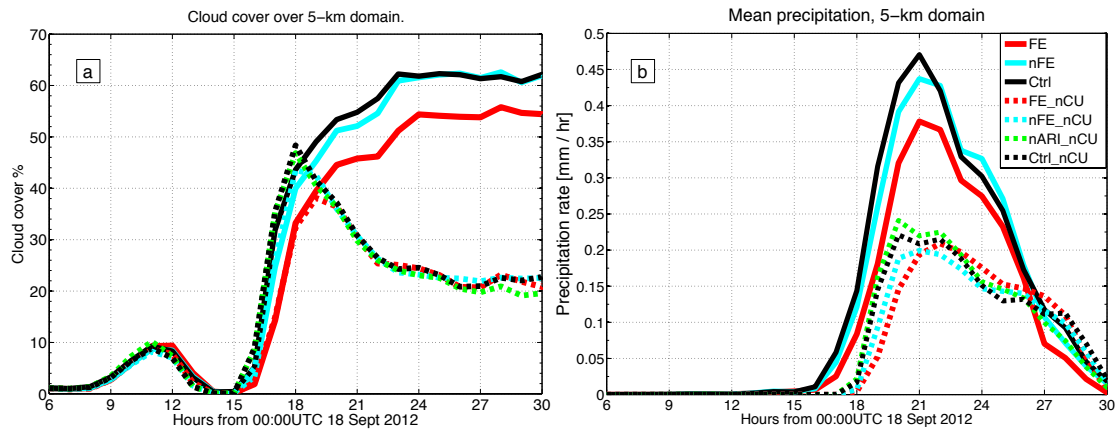


Figure 4. Cloud cover and precipitation over 5 km domain on 18 September~2012, comparing impact of biomass burning aerosol with the use of convective parameterisation. (a) shows percentage of domain covered by cloud, (b) mean precipitation rate over 5 km domain. Solid lines show simulations with convective parameterisation on, dashed line with the convective parameterisation off.

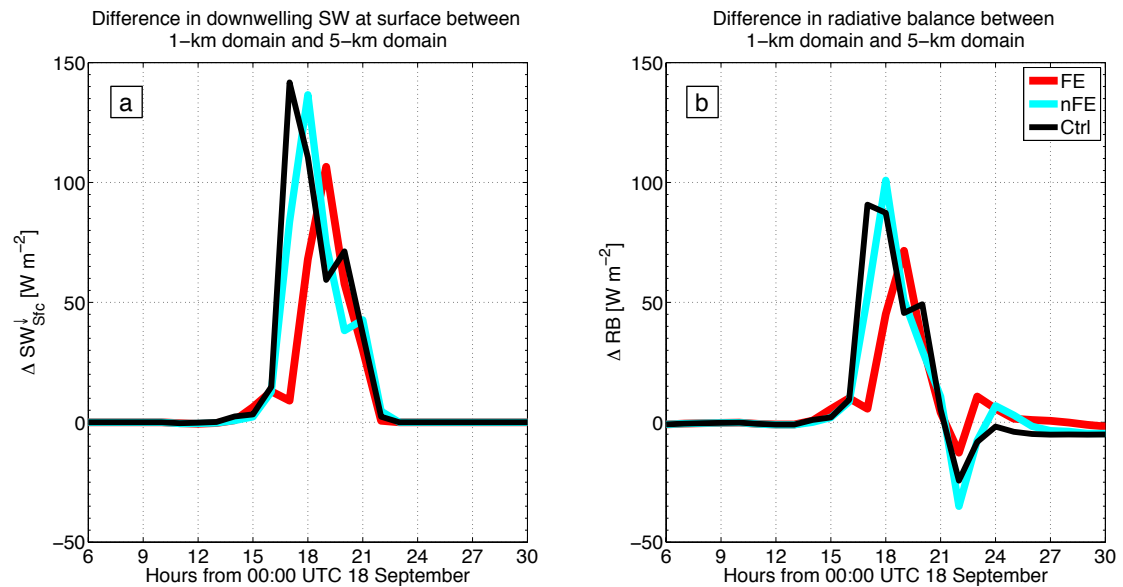


Figure 5. Comparing changes to downwelling SW radiation and radiative balance due to horizontal resolution for 18 September 2012. (a) Difference in downwelling SW radiation at surface between the 1 km domain and same region covered by the 5 km domain. (b) Difference in net radiative balance between 1 km domain and same region covered by 5 km domain.

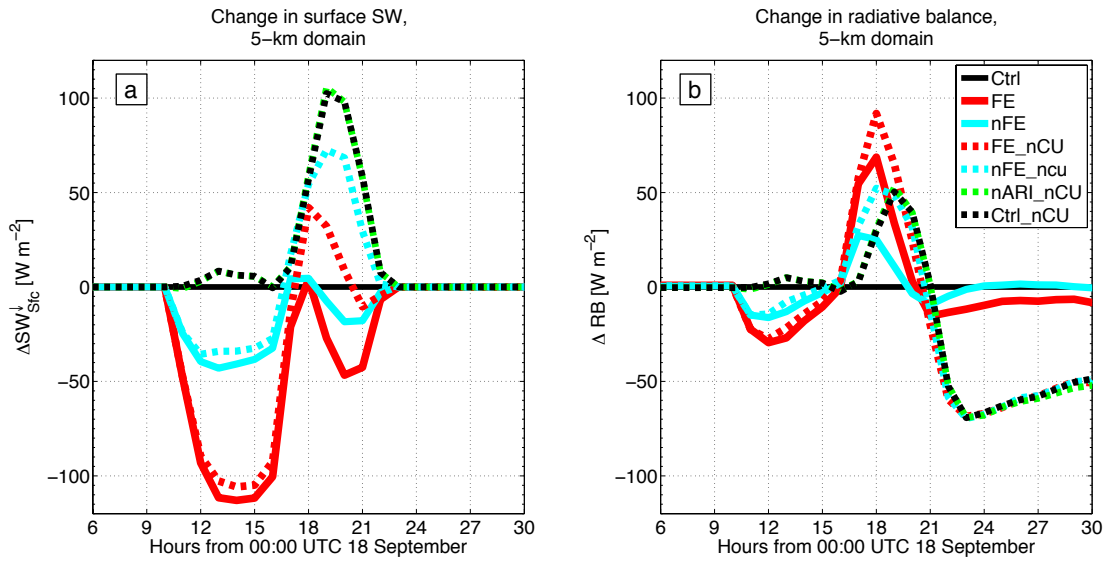


Figure 6. Comparing changes to radiative balance due to aerosol fields and convective parameterisation over the 5 km domain for 18 September 2012. (a) Difference in downwelling SW radiation at surface to the Ctrl scenario. (b) Change in net radiative balance from the Ctrl scenario. Solid lines for runs with convective parameterisation turned on, dashed lines with convective physics parameterisation turned off.

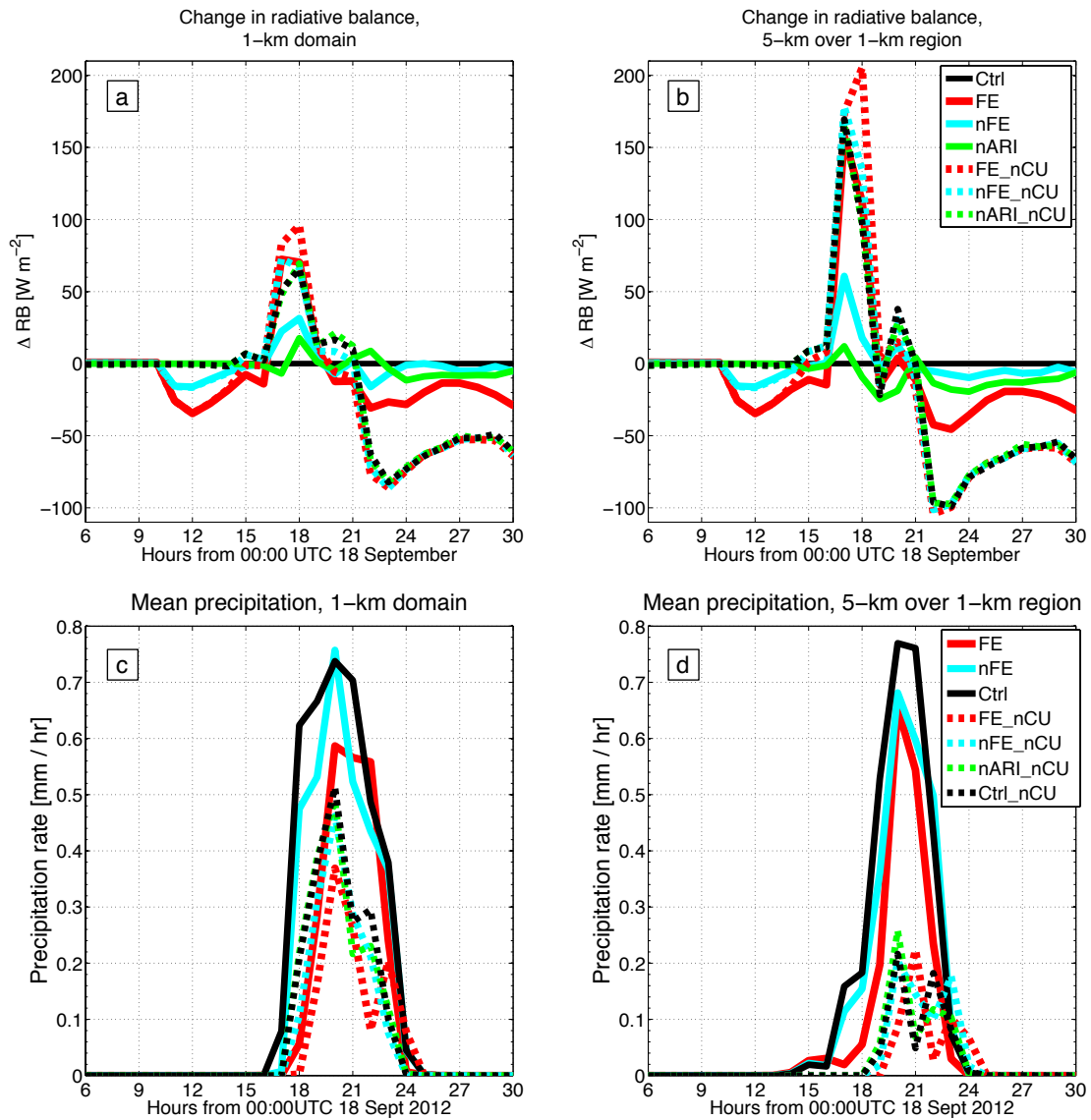


Figure 7. Net radiative balance and mean precipitation rate on 18 September 2012, over the 1 km domain region, comparing aerosol effects to use of convective parameterisation on the 5 km domain. (a) average ΔRB over the 1 km domain, (b) average ΔRB from the 5 km domain over the region covered by the 1 km domain. (c) mean precipitation rate over the 1 km domain, (d) mean precipitation rate from the 5 km domain over the region covered by the 1 km domain. Solid lines for runs with convective parameterization turned on in the 5 km domain, dashed lines with convective parameterisation turned off